ChemComm

Accepted Manuscript

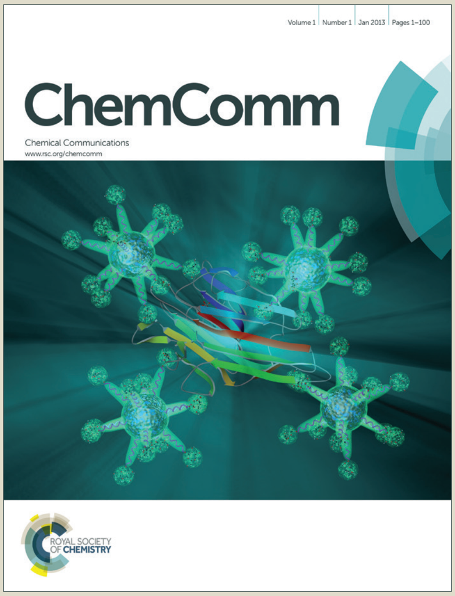

ROYAL SOCIETY OF CHEMISTRY

www.rsc.org/chemcomm

ChemComm RSCPublishing

COMMUNICATION

The B_{32} cluster has the most stable bowl structure with a remarkable heptagonal hole

Cite this: DOI: 10.1039/x0xx00000x

Truong Ba Tai* and Minh Tho Nguyen*

Received 00th January 2015,
Accepted 00th January 2015

DOI: 10.1039/x0xx00000x

www.rsc.org/chem.comm

The neutral B_{32} exhibits a aromatic and bowl structure containing one heptagonal hole, while two anionic species, one bowl structure and one quasi-planar structure, are almost degenerate in energy. These findings not only give more insight into the structural feature of boron clusters, but also a key result to explain the presence of heptagonal holes in the fullerene B_{40}.

Boron clusters continue to attract great interest in part due to the conundrum of their structural characteristics.[1-5] While the growth mechanism and bonding motif of atomic clusters of most elements are simple, the characteristics of boron clusters are unpredictably complex and remain a great challenge for both theory and experiment. Small boron clusters B_n with $n \leq 19$ were found to have quasi-planar and planar structures containing triangular B_3 units.[6,7] A few larger clusters B_{2n} such as B_{20}, B_{22}, B_{24} and B_{32} were reported to exhibit tubular forms in which two *n*-membered rings are connected together in the antiprism bonding motif.[8-11] This bonding motif was expected to be presented in larger clusters since similar structural characteristics were observed for cationic boron clusters B_n^+ with n = 16-25.[12] On the other hand, boron bulk materials such as boron nanosheets, all-boron fullerenes are formed on the basis of triangular B_3 units and contain either pentagonal or hexagonal holes.[13-15] The presence of pentagonal and hexagonal holes in these materials was very interesting, but not observed in small sized clusters. Recent findings are useful to provide us with more insight into such a problem.

Based on theoretical studies carried out by quantum chemical calculations, we found that the B_{30} cluster is an aromatic bowl structure containing one central pentagonal hole.[16] This species is proposed as a stable structural unit that eventually leads to the stable buckyballs B_{80} and B_{92}. Wang and coworkers[17] recently reported a bowl B_{36} containing one central hexagonal hole. The presence of a six-membered hole in B_{36} gave more evidence about the existence of boron nanosheets theoretically proposed earlier.[13] The most recent explorations pointed out that the B_{38} and B_{40} clusters are intriguing all-boron fullerenes. The B_{38} can be considered as a transition size between two-dimensional (2D) and three-dimensional (3D) boron clusters since there is competition in energy between the fullerene and a quasi-planar structure containing two hexagonal rings.[18,19] More interestingly, while the fullerene B_{38} contains four hexagonal holes, the B_{40} contains two hexagonal holes and four heptagonal holes.[20,21] A question thus emerges as to whether a heptagonal hole cluster could be stable. Additionally, since both B_{30} and B_{36} are bowled structures, is the tubular form a real global minimum of B_{32}? In the present work, we set out to tackle these basic problems of boron clusters.

We performed the search for the global minima of the cluster B_{32} in both neutral and anionic states using DFT and MO computational methods. We interestingly found that the neutral B_{32} is actually a bowl structure containing one heptagonal hole (Figure 1), rather than a double-ring structure as previously reported.[11] Moreover, this bowl B_{32} has an aromatic character. These findings not only end the long controversy over structural characteristics of the B_{32}, but also play a key role to explain the presence of heptagonal holes in the fullerene B_{40}. Importantly, the existence of a series of boron clusters containing 5-, 6- and 7-membered holes suggests a new family of boron clusters containing holes that are similar to the family of [*n*]-circulenes of hydrocarbons.

We performed an unbiased search for possible B_{32} structures by using a stochastic search method that was recently implemented by us.[22] The local minima with relative energies of 0.0-5.0 eV were further optimized using several density functionals including the TPSSh, PBE and PBE0 functionals, with the 6-311+G(d) basis set. Our calculations pointed out that the basis set 6-311+G(d) provides realistic computed results which is comparable to those obtained at the larger basis set def2-TZVP (Table S3, supplementary information). Finally, the calculations of single-point electronic energies for four lowest-lying isomers of the B_{32} cluster were performed using the coupled-cluster theory CCSD(T)/6-31G(d) and CCSD(T)/6-311G(d) levels at the TPSSh/6-311+G(d) optimized geometries. Due to the limit of our computer resources, the anionic species B_{32}^- are calculated using the UCCSD(T)/6-31G(d) method. Our benchmark on the B_6 clusters showed that this basis set can provide realistic relative energies for boron clusters that are comparable to those derived using the larger basis sets, including 6-311G(d), 6-311+G(d) and aug-cc-pVTZ (Table S4, supplementary information).

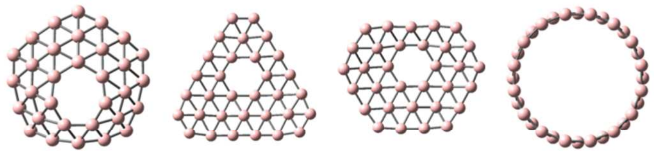

32n.1	**32n.2**	**32n.3**	**32n.4**
0.00 (0.00)	0.31 (0.31)	0.34 (0.43)	0.28 (0.17)
{0.08, 0.20, 0.56}	{0.36, 0.65, 0.93}	{0.45, 0.48, 0.98}	{0.00, 0.00, 0.00}

a) Shapes and relative energies of the neutral clusters B_{32}

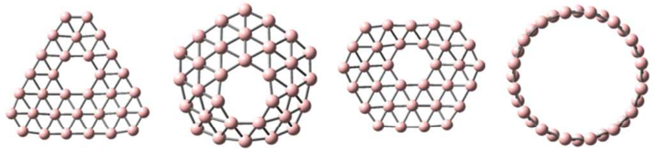

32a.1	**32a.2**	**32a.3**	**32a.4**
0.00	0.07	0.29	0.53
{0.00, 0.00, 0.32}	{0.28, 0.07, 0.50}	{0.38, 0.01, 0.56}	{0.17, 0.01, 0.00}

b) Shapes and relative energies of the anionic clusters B_{32}^-

Figure 1 Shapes and relatives energy of a) neutral B_{32} and b) anionic B_{32}^- clusters. The energy values in eV are calculated using CCSD(T)/6-31G(d) and CCSD(T)/6-311G(d) (in parentheses). The values in curly bracket are computed using the PBE0, PBE and TPSSh functionals, respectively.

Our computed DFT results show that the tubular form **32n.4** (C_{16}, ^1A) was the most stable isomer but it is only 0.08 eV more stable than **32n.1** (PBE0/6-311+G(d), Figure 1a). However, at CCSD(T) levels, the isomer **32n.1** (C_s, $^1A'$) containing one heptagonal ring is now found to be the most stable structure and is about 0.17 eV more stable than **32n.4**. Two quasi-planar structures **32n.2** (C_1, ^1A) and **32n.3** (C_1, ^1A) are also located on the energy landscape of B_{32} but are 0.31 and 0.34 eV higher in energy as compared to the global minimum **32n.1**. These results are quite remarkable since stable 2D boron clusters containing seven-membered ring have never been observed before. It is worthy to note that the quasi-planar 2D structures without defect holes are found for small boron clusters B_n with n = 2-19. While the tubular double-ring form tends to be favoured for B_{20}-B_{24}, as stated above, the bowl structures containing pentagonal and hexagonal were found for the clusters B_{30} and B_{36}. The present results emphasize that the hole defect structures seem to be a common bonding motif for B_n with n = 30-36, since both B_{38} and B_{40} are 3D fullerenes.

Similar observations were found for the anionic B_{32}^- cluster. At the TPSSh/6-311+G(d) level, the isomer **32a.4** (C_{8v}, $^2A_1$) is the lowest isomer. The energy ordering of isomers is reversed when higher accuracy computational methods were used. At the CCSD(T)/6-31G(d) level, **32a.1** (C_1, ^2A) which is the anionic form of **32n.2,** is the most stable isomer (Figure 1b). The heptagonal hole defect structure **32a.2** (C_s, $^2A''$) is also located as a stable isomer and is only ~0.07 eV less stable than the first.

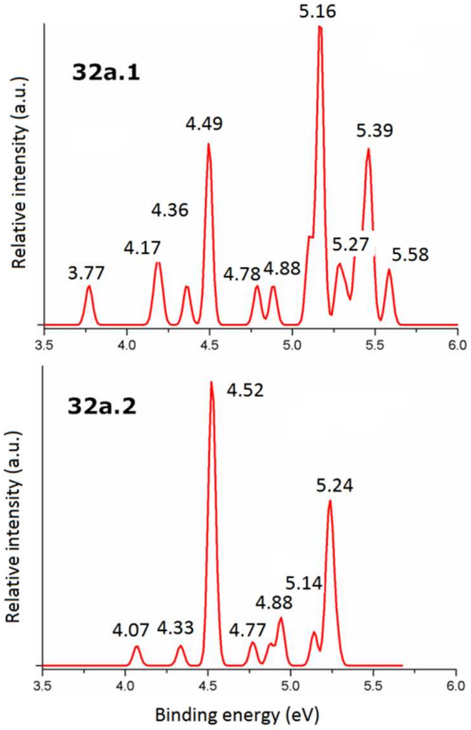

Figure 2 Photoelectron spectrum of **32a.1** and **32a.2** simulated by using TD-TPSSh/6-311+G(d) method

In order to verify the reality of computational methods used, the T1 diagnostic values are calculated using CCSD(T) methods. The values given in Table S5, supplementary information showed that the T1 diagnostic values of anionic species B_{32}^- are in range of 0.023 ÷ 0.035, while those of neutral species B_{32} vary in range of 0.017 ÷ 0.029. These values are comparable to the values of 0.04 for opened shell systems and 0.02 for close shell systems where the electronic structure of system has single-referential nature. Consequently, the computational methods used in this report can provide realistic computed results for the boron clusters B_{32}.

The vertical detachment energies (VDEs) of the lowest-lying isomers **32a.1** and **32a.2** were calculated using time-dependent TD-DFT method. The calculated values are given in Table S1 and S2 of the Supplementary information, while the simulated photoelectron spectra are shown in Figure 2. The adiabatic (ADE) and vertical (VDE) detachment energies of **32a.1** and **32a.2** equal to 3.6/3.8 and 3.1/3.2 eV, respectively. As shown in Figure 2, there are overlaps between peaks of **32a.1** and **32a.2** in the range of 4.3 to 5.2 eV. These characteristics are similar to those of anionic boron clusters previous reported where many degenerate in energy isomers are present in their experimental PES spectra. This indicates that both isomers **32a.1** and **32a.2** co-exist as stable isomers of the

B_{32}^- anion. We should note that there may be the existence of other stable anionic isomers on the experimental PES spectrum of the B_{32}^-.

Aromaticity and bonding characteristics of boron clusters remains an attractive subject. We now examine the aromatic feature of B_{32} by using the nucleus independent chemical shift (NICS) calculations,[23] and the model of disk-aromaticity.[24] While the first index is popularly used to evaluate molecular aromaticity, the latter was recently proposed by us and effectively applied to boron clusters such as B_{20}^-, B_{30}, B_{36} and also polycyclic compounds.[16,24,25] Within the framework of the disk aromaticity model, a free particle is moved on a plane encircled by infinite walls. The energy of particle can be quantified by solving its Schrödinger equation using Bessel functions as follows:

$$E = \frac{\hbar^2 \left(a_{m,n}\right)^2}{2\mu R^2}\ with\!: n = 1,2,3, \ldots m = 0, \pm 1, \pm 2, \pm 3 \quad (1)$$

where $a_{m,n}$ quantities are dimensionless, n is a radial quantum number that counts the zeroes, and m is the rotational quantum numbers are usually denoted by Greek letters as $m = \sigma, \pi, \delta, \phi, \gamma\ldots$ States with non-zero values for m will be twofold degenerate. The lowest eigenstates in ascending order are 1σ, 1π, 1δ, 2σ etc (more detail about the model can be seen at ref. 16 and 24 and Supplementary Information). We consider that the systems containing the number of 2, 6, 10, 12, 16… electrons will exhibit a disk-aromaticity. Oppositely, the systems containing number of 4, 8, 14, 18… electrons will be disk-antiaromatic.

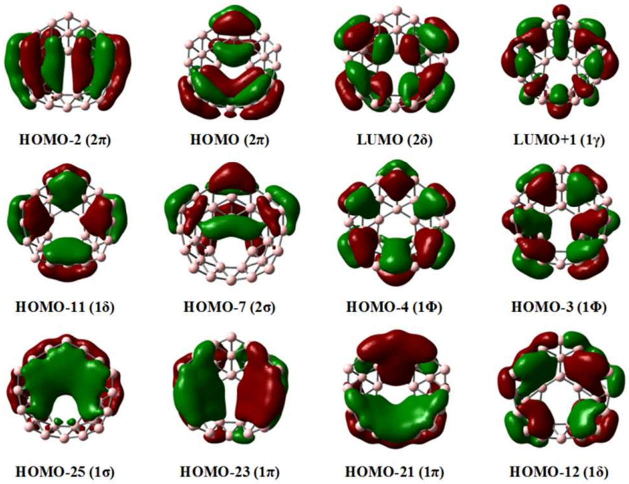

Figure 3 Shapes of π-molecular orbitals of the neutral **32n.1**

Shapes of π molecular orbitals (MOs) of the global minimum reveal that the bowl **32n.1** contains 20 valence π-electrons that fully occupy 10 π-orbitals (HOMO, HOMO-2, HOMO-3, HOMO-4, HOMO-7, HOMO-11, HOMO-12, HOMO-21, HOMO-23 and HOMO-23) in ascending order of $1\sigma^2 1\pi^4 1\delta^4 2\sigma^2 1\varphi^4 2\pi^4$ (Figure 3). Accordingly, **32n.1** exhibits a disk-aromatic feature similar to the MO configuration of B_{30}. In the anionic state, the excess electron will occupy the 2δ-LUMO of the neutral **32n.1**. Consequently, the anion **32a.2** will be antiaromatic species because its π-electrons fulfil only one of two degenerate 2δ-MOs with the electronic configuration $1\sigma^2 1\pi^4 1\delta^4 2\sigma^2 1\varphi^4 2\pi^4 2\delta^1$.

NICS calculations agree well with the above discussion. The NICS values were calculated at the centre of heptagonal hole of **32n.1** and **32a.2**. The ghost atoms were placed at positions of 0, 1, 2, and 3 Å along z-axis that is normal to the plane containing the heptagonal hole. The NICS values of **32n.1** are highly negative ($NICS_{zz}(0) = -9.4$, $NICS_{zz}(1) = -37.5$, $NICS_{zz}(2) = -50.7$ and $NICS_{zz}(3) = -43.6$), while the NICS values of **32a.1** are highly positive ($NICS_{zz}(0) = +47.6$, $NICS_{zz}(1) = +40.4$, $NICS_{zz}(2) = +13.2$ and $NICS_{zz}(3) = +2.0$). Thus the **32n.1** exhibits a pronounced aromatic character, and the **32a.2** is anti-aromatic. These aromatic features can be one of main reasons that lead to a high thermodynamic stability of **32n.1**.

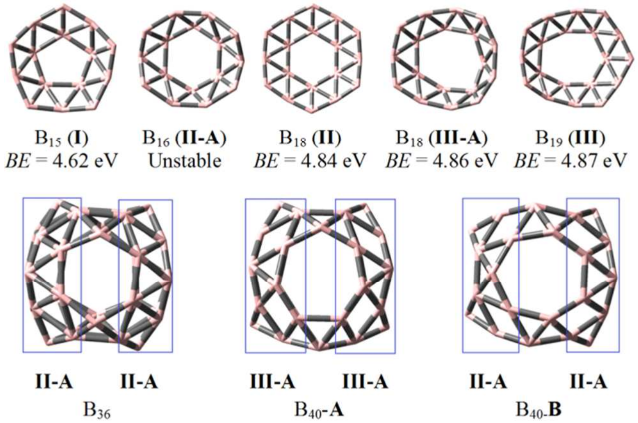

Figure 4 Shapes of small units containing pentagonal **I**, hexagonal **II** and **II-A**, and heptagonal holes **III** and **III-A**, and the fullerenes B_{36} and B_{40}

The existence of bowl structures containing pentagonal, hexagonal and heptagonal holes is intriguing in boron chemistry. Recently, a breakthrough was marked when the the existence of all-boron fullerene B_{40} containing 4 heptagonal holes and 2 hexagonal holes at both neutral and anionic states[21] was demonstrated. To gain more insights into these structural characteristics, we examined further on the smaller species **I-III** displayed in Figure 4. All structures considered were optimized at the TPSSh/6-311+G(d) level and their harmonic vibrational frequencies and average binding energies (*BE*) were calculated at the same level. Although being less stable than the corresponding global minima, all structures **I-III** are located as local minima without imaginary frequency. The binding energies are consistently increased from **I** to **III** as size of boron clusters increased. Stabilizing **I**, **II** and **III** by surrounding B-atoms results in larger clusters B_{30}, B_{36} and B_{32}, respectively. This growth motif can be expected at other sizes in series of intermediate-sized boron clusters B_n.

More interestingly, our calculations show that the **III-A** containing a heptagonal hole is also located on the energy landscape of cluster B_{18} and even more stable than **II**.

Oppositely, the **II-A** is unstable and its geometry is distorted to another form after geometry optimization. These observations indicate that the fullerene B_{40} is formed by connecting two units **III-A** together to the motif **B_{40}-A**. The growth motif **B_{40}-B** in which two unit **II-A** are connected each other is not preferred because of the inherent instability of **II-A**. This gives the reason for why the fullerene B_{36} is much less stable than the corresponding bowl form.[17,18]

Conclusions

In conclusion, we performed a theoretical investigation of structural and aromatic characteristics of the B_{32} clusters in both neutral and anionic states. We found that the neutral B_{32} exhibits a bowl and aromatic structure **32n.1** containing one heptagonal hole, while in the anionic state both isomers **32a.1** and **32a.2** are almost degenerate in energy. These findings not only give more insight into the structural feature of intermediate-sized boron clusters, but also a key result to explain the presence of heptagonal holes in the fullerene B_{40}. In addition, the existence of a series of boron clusters containing 5-, 6- and 7-membered holes foreshadows a new family of boron clusters containing holes that are similar to family of [*n*]-circulenes of hydrocarbons. We would hope that relevant experimental studies can be performed in a near future on the intriguing B_{32} clusters.

Notes and references

[a]Department of Chemistry, University of Leuven, Celestijnenlaan 200F, B-3001 Leuven, Belgium.
E-mails: truong.batai@chem.kuleuven.be; minh.nguyen@chem.kuleuven.be

Electronic Supplementary Information (ESI) available:. See DOI: 10.1039/c000000x/

1 I. Boustani, Z. Zhu and D. Tomanek, *Phys. Rev. B.*, 2011, **83**, 193405
2 (a) W. L. Li, Q. Chen, W. J. Tian, H. Bai, Y. F. Zhao, H. S. Hu, J. Li, H. J. Zhai, S. D. Li and L. S. Wang, *J. Am. Chem. Soc.*, 2014, **136**, 12257; (b) H. J. Zhai, A. N. Alexandrova, K. A. Birch, A. I. Boldyrev and L. S. Wang, *Angew. Chem. Int. Ed.*, 2003, **42**, 6004; (c) H. J. Zhai, B. Kiran, J. Li and L. S. Wang, *Nature Materials*, 2003, **2**, 827
3 (a) D. Moreno, S. Pan, L. L. Zeonjuk, R. Islas, E. Osorio, G. M. Guajardo, P. K. Chattaraj, T. Heine and G. Merino. *Chem. Commun*, 2014, **50**, 8140; (b) J. O. C. Jimenez-Halla, R. Islas, T. Heine and G. Merino, *Angew. Chem. Int. Ed.* 2010, **49**, 5668; (c) G. Merino and T. Thomas, *Angew. Chem. Int. Ed.* 2012, **51**, 10226
4 (a) S. R. Reddy and S. Mahapatra, *J. Chem. Phys*., 2012, **136**, 024322; (b) S. R. Reddy and S. Mahapatra, *J. Chem. Phys*. 2012, **136**, 024323
5 J. Zhang, A. Sergeeva, M. Sparta and A. N. Alexandrova, *Angew. Chem. Int. Ed.* 2012, **51**, 8512
6 (a) C. Romanescu, D. J. Harding, A. Fielicke and L. S. Wang, *J. Chem. Phys*. 2012, **137**, 014317; (b) A. N. Alexandrova, A. I. Boldyrev, H. J. Zhai and L. S. Wang, *Coord. Chem. Rev*. 2006, **250**, 2811 and references therein
7 (a) T. B. Tai, D. J. Grant, M. T. Nguyen and D. A. Dixon, *J. Phys. Chem. A,* 2010, **114**, 994; (b) T. B. Tai, M. N. Tam and M. T. Nguyen, *Chem. Phys. Lett*. 2012, **530**, 71; (c) T. B. Tai, N. M. Tam and M. T. Nguyen, *Theor. Chem. Acc*. 2012, **131**, 1241
8 B. Kiran, S. Bulusu, H. J. Zhai, S. Yoo, X. C. Zeng, and L. S. Wang, *PNAS*, 2005, **102**, 961
9 B.C. Hikmat, B. Tunna and R. Z. Rajendra, *J. Phys. B: At.Mol.Opt.Phys.,* 2012, **45**, 225101
10 S. Chacko, D. G. Kanhere and I. Boustani, *Phys. Rev. B*, 2003, **68**, 035414
11 (a) I. Boustani, *J. Solid State Chem*, 1997, **133**, 182; (b) I. Boustani, A. Rubio and J. A. Alonso, *Chem. Phys. Lett*., 1999, **311**, 21; (c) Y. Zhao, M, Zhang, B. Chen, J. Zhang and C-C. Sun, *Theochem*, 2006, **759**, 25
12 E. Oger, N. R. M. Crawford, R. Kelting, P. Weis, M. M. Kappes and R Ahlrichs, *Angew. Chem. Int. Ed.* 2007, **46**, 8503
13 X, Wu, J. Dai, Y. Zhao, J. Zhou, and X. C. Zeng, *ACS NANO*, 2012, **6**, 7443
14 H. Tang, S. Ismail-Beigi, *Phys. Rev. Lett*., 2007, **99**, 115501
15 N. G. Szwacki, A. Sadrzadeh and B. I. Yakobson, *Phys. Rev. Lett*., 2007, **98**, 166804
16 T. T. Tai, L. V. Duong. H. T. Pham, D. T. T. Mai and M. T. Nguyen, *Chem. Commun*, 2014, **50**, 1558
17 Z. A. Piazza, H. S. Hu, W. L. Li, Y. F. Zhao, J. Li and L. S. Wang, *Nature Commun*. 2014, **5**, 3113
18 J. Lu, Y. Wang, L. Zhu and Y. Ma, *Nanoscale*, 2014, **6**, 11692
19 T. B. Tai and M. T. Nguyen, *Nanoscale*, 2015, **7,** 3316.
20 H. T. Pham, L. V. Duong, N. M. Tam, M.P. P. Ho, and M. T. Nguyen, *Chem. Phys. Lett*, 2014, **608**, 295
21 H. J. Zhai, Y. F. Zhao, W. L. Li, Q. Chen, H. Bai, H. S. Hu, Z. A. Piazza, W. J. Tian, H. G. Lu, Y. B. Wu, Y. W. Mu, G. F. Wei, Z.P. Liu, J. Li, S. D. Li, and L. S. Wang, *Nature Chemistry*, 2014, *6*, 727
22 T. B. Tai and M. T. Nguyen, *J. Chem. Theory. Comput.*, 2011, **7**, 1119
23 P. v. R. Schleyer, H. Jiao, N. J. R. V. E. Hommes, V. G. Malkin and O. L. Malkina, *J. Am. Chem. Soc*. 1997, **119**, 12669
24 (a) T. B. Tai, A. Ceulemans and M. T. Nguyen, *Chem. Eur-J.* 2012, **18**, 4510; (b) T. B. Tai, R. W. A. Havenith, J. L. Teunissen, A. R. Dok, S. D. Hallaert, M. T. Nguyen and A. Ceulemans, *Inorg. Chem*., 2013, **52**, 10595
25 T. B. Tai, V. T. T. Huong and M. T. Nguyen, *Top. Heterocyc. Chem* 2014, **38**, 161.